Hybrid high-order (HHO) method for numerical simulation of seismo-acoustic wave propagation

Author : Romain Mottier[§†‡] (PhD student)   **Supervision** : Alexandre Ern[†‡], Laurent Guillot[§]

[†] École nationale des ponts et chaussées (ENPC - CERMICS: `https://cermics-lab.enpc.fr/`)
[§] Commissariat à l'énergie atomique et aux énergies alternatives (CEA: `https://www.cea.fr/english`)
[‡] Institut national de recherche en sciences et technologies du numérique (INRIA - SERENA: `https://team.inria.fr/serena/`)

Context and issues - Coupling of acoustic and elastic wave equations

Goals

- Accurate simulation of seismo-acoustic waves through **heterogeneous domains with complex geometries**
- Treatment of realistic cases of interest
  - **High computational costs**

Issues

- High-order precision needed to accurately capture waves
  - **Hybrid discontinuous methods (HDG/HHO)**

- **Acoustic wave equations:**
$$\begin{cases} \rho_F \partial_t \boldsymbol{v}^F(t) + \nabla p(t) = \boldsymbol{0} \\ \frac{1}{\kappa}\partial_t p(t) + \nabla \cdot \boldsymbol{v}^F(t) = g(t) \end{cases}$$
- **Elastic wave equations:**
$$\begin{cases} \partial_t \boldsymbol{\varepsilon}(t) - \nabla^s \boldsymbol{v}^S(t) = \boldsymbol{0} \\ \rho_S \partial_t \boldsymbol{v}^S(t) - \nabla \cdot (\boldsymbol{\mathcal{C}} : \boldsymbol{\varepsilon}(t)) = \boldsymbol{f}(t) \end{cases}$$
- **Coupling conditions:**
$$\begin{cases} [\![\boldsymbol{v}(t) \cdot \boldsymbol{n}_\Gamma]\!]_\Gamma = 0 \\ (\boldsymbol{\mathcal{C}} : \boldsymbol{\varepsilon}(t)) \cdot \boldsymbol{n}_\Gamma = p(t)\boldsymbol{n}_\Gamma \end{cases}$$

Application of HHO method to seismo-acoustic coupling

- **Approximation spaces:**
  - **Acoustic domain:** $\boldsymbol{v}^F \longrightarrow \mathrm{dG}(k)$, $p \longrightarrow \mathrm{HHO}(k', k)$
  - **Elastic domain:** $\boldsymbol{\varepsilon} \longrightarrow \mathrm{dG}(k)$, $\boldsymbol{v}^S \longrightarrow \mathrm{HHO}(k', k)$

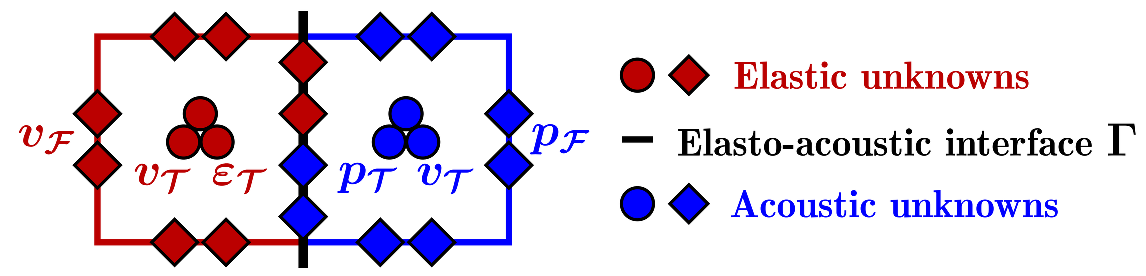

Fig. 1: Elasto-acoustic unknowns with a mixed-order discretization ($k' = k + 1 = 2$)

- **Algebraic realization:**

$$\begin{bmatrix} M^v_{\mathcal{TT}} & 0 & 0 & 0 & 0 & 0 \\ 0 & M^F_{\mathcal{TT}} & 0 & 0 & 0 & 0 \\ 0 & 0 & 0 & 0 & 0 & 0 \\ 0 & 0 & 0 & M^\varepsilon_{\mathcal{TT}} & 0 & 0 \\ 0 & 0 & 0 & 0 & M^S_{\mathcal{TT}} & 0 \\ 0 & 0 & 0 & 0 & 0 & 0 \end{bmatrix} \begin{bmatrix} \partial_t V^F_\mathcal{T} \\ \partial_t P_\mathcal{T} \\ \partial_t P_\mathcal{F} \\ \partial_t S_\mathcal{T} \\ \partial_t V_\mathcal{T} \\ \partial_t V_\mathcal{F} \end{bmatrix} + \begin{bmatrix} 0 & -G_\mathcal{T} & -G_\mathcal{F} & 0 & 0 & 0 \\ G^\dagger_\mathcal{T} & \Sigma^F_{\mathcal{TT}} & \Sigma^F_{\mathcal{TF}} & 0 & 0 & 0 \\ G^\dagger_\mathcal{F} & \Sigma^F_{\mathcal{FT}} & \Sigma^F_{\mathcal{FF}} & 0 & 0 & C_\Gamma \\ 0 & 0 & 0 & 0 & -E_\mathcal{T} & -E_\mathcal{F} \\ 0 & 0 & 0 & E^\dagger_\mathcal{T} & \Sigma^S_{\mathcal{TT}} & \Sigma^S_{\mathcal{TF}} \\ 0 & 0 & -C^\dagger_\Gamma & E^\dagger_\mathcal{F} & \Sigma^S_{\mathcal{FT}} & \Sigma^S_{\mathcal{FF}} \end{bmatrix} \begin{bmatrix} V^F_\mathcal{T} \\ P_\mathcal{T} \\ P_\mathcal{F} \\ S_\mathcal{T} \\ V^S_\mathcal{T} \\ V^S_\mathcal{F} \end{bmatrix} = \begin{bmatrix} 0 \\ G_\mathcal{T} \\ 0 \\ 0 \\ F_\mathcal{T} \\ 0 \end{bmatrix}$$

- **Mechanical energy of the scheme:** $\mathcal{E}_h(t) := \mathcal{E}_h^S(t) + \mathcal{E}_h^F(t)$ with

$$\mathcal{E}_h^F(t) := \frac{1}{2}\|\boldsymbol{v}^F_\mathcal{T}(t)\|^2_{\boldsymbol{L}^2(\rho_F;\Omega_F)} + \frac{1}{2}\|p_\mathcal{T}(t)\|^2_{L^2(\frac{1}{\kappa};\Omega_F)}, \qquad \mathcal{E}_h^S(t) := \frac{1}{2}\|\boldsymbol{v}^S_\mathcal{T}(t)\|^2_{\boldsymbol{L}^2(\rho_S;\Omega_S)} + \frac{1}{2}\|\boldsymbol{\varepsilon}_\mathcal{T}(t)\|^2_{\boldsymbol{L}^2(\boldsymbol{\mathcal{C}};\Omega_S)}$$

- **Semi-discrete energy conservation of the scheme:**

$$\mathcal{E}_h(t) = \mathcal{E}_h(0) + \int_0^t \Big[(\boldsymbol{f}(\alpha), \boldsymbol{v}^S_\mathcal{T}(\alpha))_{\boldsymbol{L}^2(\Omega_S)} + (g(\alpha), p_\mathcal{T}(\alpha))_{L^2(\Omega_F)} - s_h^S(\hat{\boldsymbol{v}}_h^S(\alpha), \hat{\boldsymbol{v}}_h^S(\alpha)) - s_h^F(\hat{p}_h(\alpha), \hat{p}_h(\alpha)) \Big] \, d\alpha$$

Propagation of an acoustic (water) pulse into an elastic medium (granite)

- **Computational parameters:**
  - **Computational domain:**
    - **Water** on the upper side
    - **Granite** on the lower side
  - **Mixed-order discretization:** $k' = k + 1 = 3$
  - **Time integration scheme:** SDIRK(3,4)
  - **Time step:** $\mathrm{dt} = 0,1 \times 2^{-9}$
  - **Homogeneous Dirichlet conditions**
  - **IC:** velocity Ricker wave in the acoustic medium:
$$\boldsymbol{v}_0^F(x,y) := \theta \exp\left(-\pi^2 \frac{r^2}{\lambda^2}\right)(x - x_c, y - y_c)^T$$

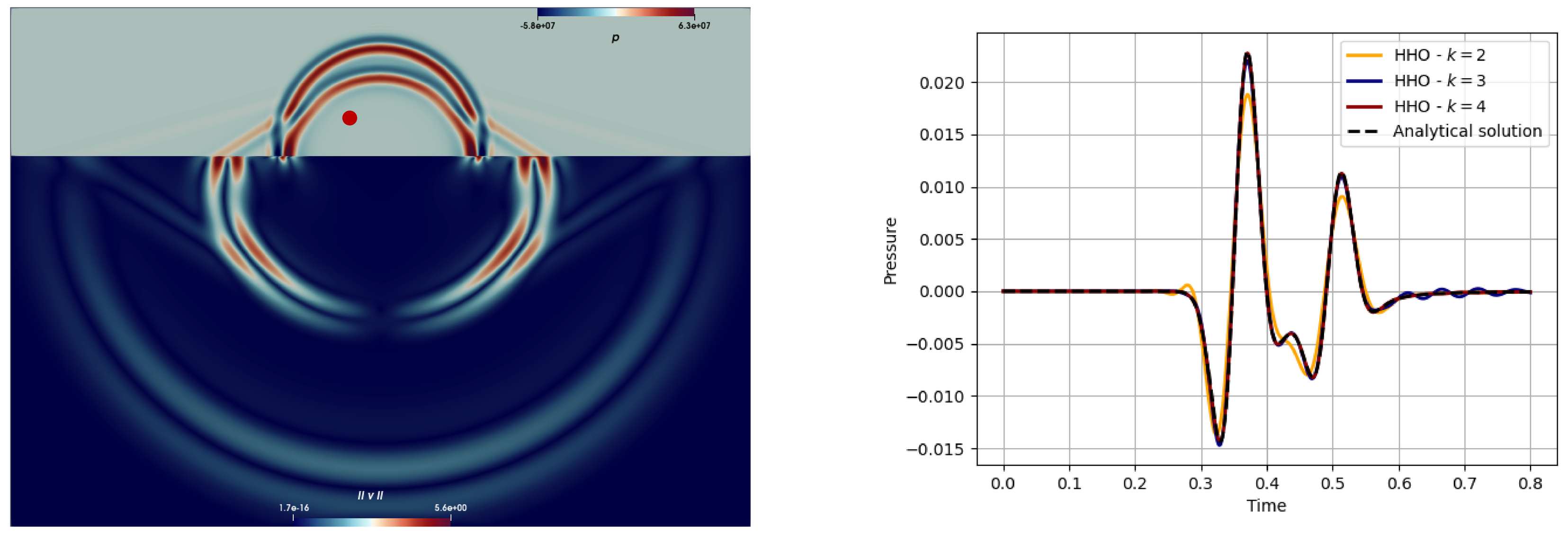

Fig. 5: Left panel: Distribution of acoustic pressure and elastic velocity norm, at $t = 0,4375$ s. Right panel: Pressure as a function of time at a sensor in the water (coarse mesh)

General principles of HHO method

- **HHO is a finite element method similar to the Hybrid Discontinuous Galerkin method (HDG)**

Design of HHO method

- **Degrees of freedom:**
  - Polynomial unknowns located in the cells (degree k') and on the faces (degree k): $\hat{\boldsymbol{u}}_h := (\boldsymbol{u}_\mathcal{T}, \boldsymbol{u}_\mathcal{F})$
  - Equal-order discretization: $k' = k$
  - Mixed-order discretization: $k' = k + 1$
- **Operators:**
  - Gradient reconstruction operator: $\nabla \boldsymbol{u} \rightarrow \mathrm{G}(\hat{\boldsymbol{u}}_h)$,
  - Stabilization operator: $\mathrm{s}(\hat{\boldsymbol{u}}_h, \hat{\boldsymbol{w}}_h)$
    - Penalty at element level to enforce weakly the matching of the trace of the cell unknown with the local face unknowns

Advantages over classical finite element methods

- **Mesh flexibility:**
  - Complex geometries
  - Unstructured and polyhedral meshes
  - Local mesh refinement
- **Local conservativity**
- **Optimal error estimates (for smooth solutions)**
- **Attractive computational costs:**
  - Global problem couples only face dofs
  - Cell dofs recovered by local post-processing

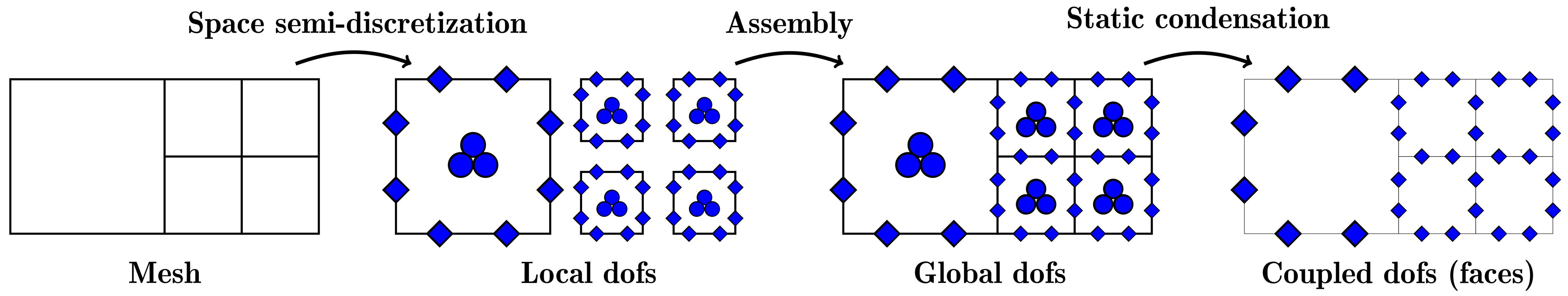

Fig. 2: Static condensation procedure

Verification on academic test cases

- **Convergence rates on sinusoïdal solutions:**
  - $\mathcal{O}(h^{k+1})$ in H^1-norm
  - $\mathcal{O}(h^{k+2})$ in L^2-norm **(superconvergence)**
- **Energy conservation:**
  - $\rho_S = \rho_F = 1$, $c_S^P = c_F^P = \sqrt{3}$, $c_S^S = 1$
  - **IC:** velocity Ricker wave in acoustic medium:
$$\boldsymbol{v}_0^F(x,y) := \theta \exp\left(-\pi^2 \frac{r^2}{\lambda^2}\right)(x - x_c, y - y_c)^T$$

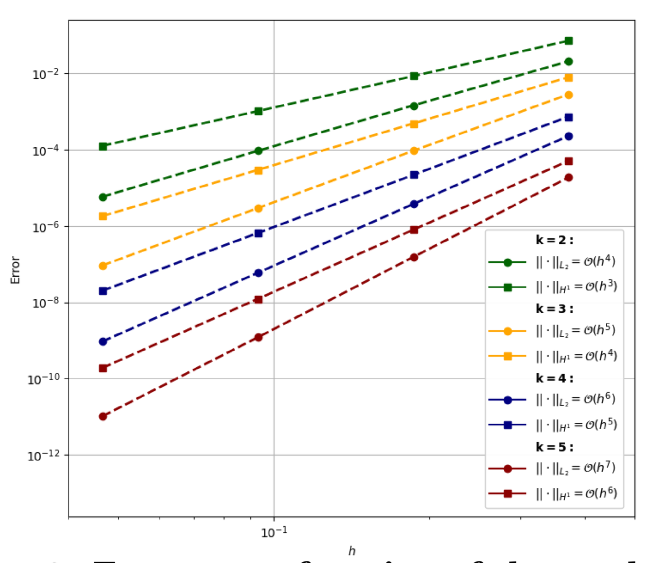

Fig. 3: Errors as a function of the mesh size with $\Delta t = 0.1 \times 2^{-5}$

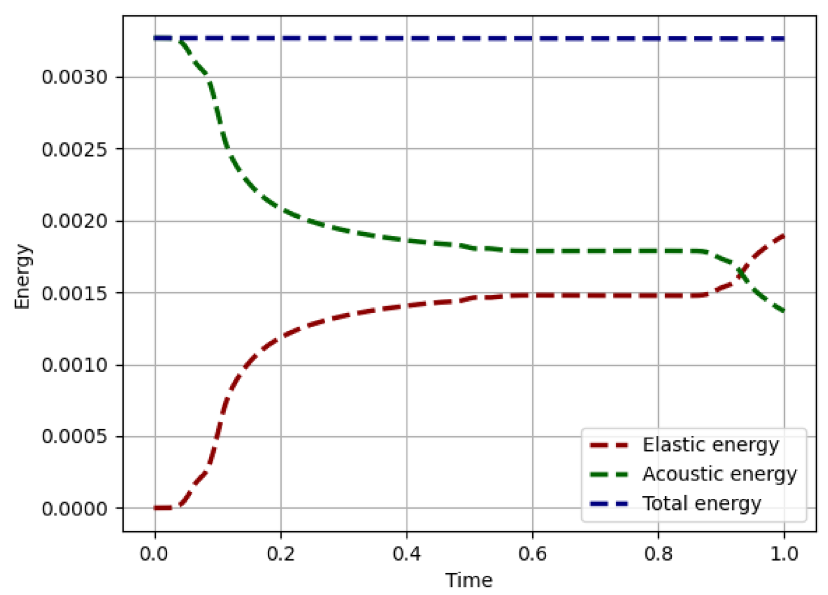

Fig. 4: Repartition of elastic and acoustic energy

Propagation of an elastic pulse in a sedimentary basin and atmosphere

- **Acoustic region:** $\rho = 1,292$ kg.m^3, $c_P = 340$ m.s^{-1}
- **Sedimentary region:** $\rho = 1200$ kg.m^3, $c_P = 3400$ m.s^{-1}, $c_S = 1400$ m.s^{-1}
- **Bedrock region:** $\rho = 5350$ kg.m^3, $c_P = 3090$ m.s^{-1}, $c_S = 2570$ m.s^{-1}

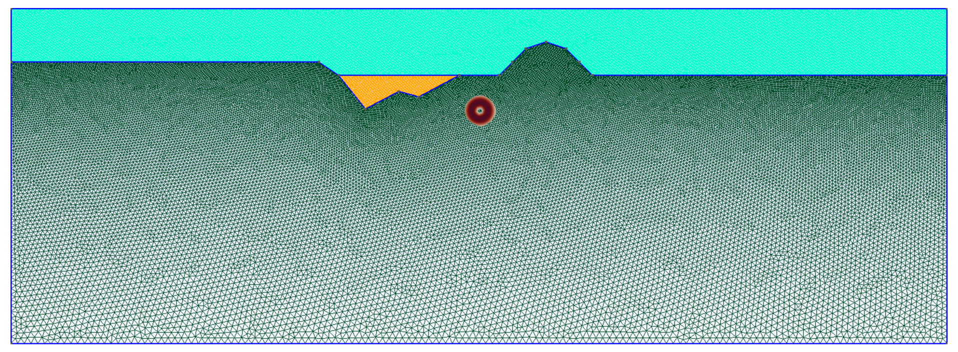

Fig. 6: Mesh of sedimentary basin and location of initial pulse

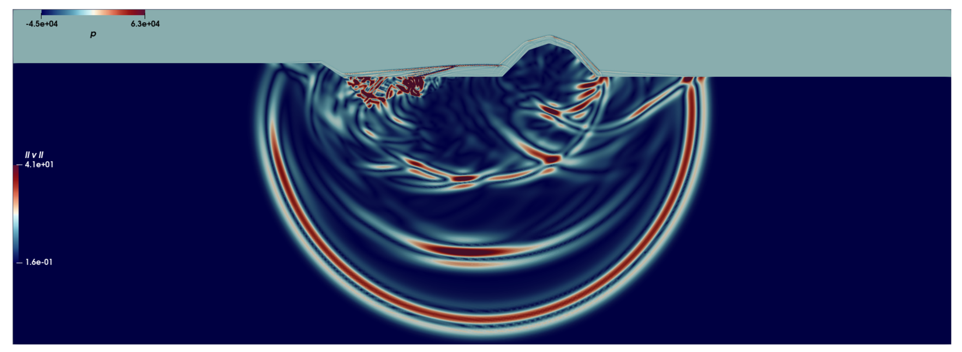

Fig. 7: Propagation through the sedimentary basin

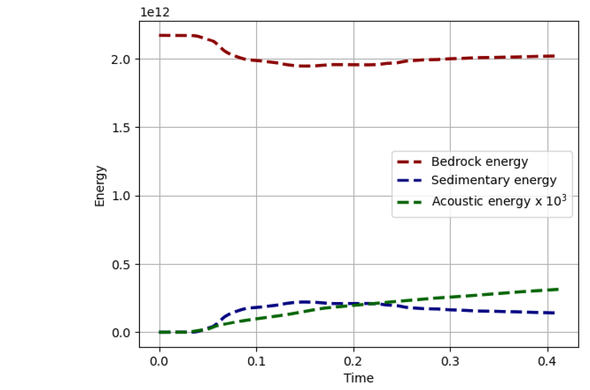

Fig. 8: Repartition of elastic and acoustic energy

- **Energy transfer enhancement above the sedimentary basin**

Some references

[1] Burman, Duran, and Ern. "Hybrid high-order methods for the acoustic wave equation in the time domain". In: *Comm. App. Math. Comp. Sci.* 4.2 (2022), pp. 597–633.
[2] Di Pietro and Ern. "A hybrid high-order locking-free method for linear elasticity on general meshes". In: *Comput. Meth. Appl. Mech. Engrg.* 283 (2015), pp. 1–21.
[3] Terrana, Vilotte, and Guillot. "A spectral hybridizable discontinuous Galerkin method for elastic-acoustic wave propagation". In: *Geophys. J. Int.* 213.1 (2017), pp. 574–602.